Aalto University

Aaltodoc
OPEN ACCESS



Author(s): Jelovica, Jasmin & Romanoff, Jani & Ehlers, Sören & Varsta, Petri

Title: Influence of weld stiffness on buckling strength of laser-welded web-core sandwich plates

Year: 2012

Version: Post print

**Please cite the original version:**

Jelovica, Jasmin & Romanoff, Jani & Ehlers, Sören & Varsta, Petri. 2012. Influence of weld stiffness on buckling strength of laser-welded web-core sandwich plates. Journal of Constructional Steel Research. Volume 77. p. 12-18. DOI: 10.1016/j.jcsr.2012.05.001.

# Influence of weld stiffness on buckling strength of laser-welded web-core sandwich plates

J. Jelovica[1*], J. Romanoff[1], S. Ehlers[2], P. Varsta[1]

[1] *Department of Applied Mechanics / Marine Technology, Aalto University School of Engineering, P.O. Box 15300, 00076 Aalto, Finland*

[2] *Department of Marine Technology, Norwegian University of Science and Technology, 7491 Trondheim, Norway*

**Abstract**

This paper investigates the influence of weld rotation stiffness on the global bifurcation buckling strength of laser-welded web-core sandwich plates. The study is carried out using two methods, the first is the equivalent single-layer theory approach solved analytically for simply supported plates and numerically for clamped plates. First-order shear deformation theory is used. The second method is the three-dimensional model of a sandwich plate solved with finite element method. Both approaches consider the weld through its rotation stiffness. The weld rotation stiffness affects the transverse shear stiffness. Plates are loaded in the web plate direction. Four different cross-sections are considered. Weld stiffness is taken from experimental results presented in the literature. The results show a maximum of 24% decrease in buckling strength. The strength was affected more in plates with high reduction of transverse shear stiffness and high bending stiffness. Furthermore, clamped plates were influenced more than simply supported. The intersection between buckling modes shifted towards higher aspect ratios, in the maximum case by 24%. The results show the importance of considering the deforming weld in buckling analysis.

**Keywords:** bifurcation buckling strength; global buckling; laser weld; rotation stiffness; shear stiffness; web core; sandwich plate.

## List of symbols

| | |
|---|---|
| $a$ | Length of the sandwich plate (m) |
| $b$ | Width of the sandwich plate (m) |
| $d$ | Distance between neutral axes of the face plates (mm) |
| $t_t$ | Thickness of top face plate (mm) |
| $t_b$ | Thickness of bottom face plate (mm) |
| $t_f$ | Thickness of face plate (mm) |
| $t_w$ | Thickness of web plate (mm) |
| $s$ | Spacing of the web plates (mm) |
| $h_c$ | Height of the sandwich plate core (mm) |
| $m$ | Number of buckling half-waves in $x$-direction |
| $n$ | Number of buckling half-waves in $y$-direction |
| $k_\theta$ | Rotation stiffness of laser weld (kN) |

[*] Corresponding author. Tel. +358 9 4702 4172; Fax: +358 9 4702 4173. *E-mail address:* jasmin.jelovica@aalto.fi

| | |
|---|---|
| $u$ | Displacement component in $x$-direction (m) |
| $v$ | Displacement component in $y$-direction (m) |
| $w$ | Deflection of the plate (m) |
| $D$ | Bending stiffness of isotropic steel plate (Nm) |
| $D_{ij}$ | Bending stiffness of sandwich plate, $i,j$ = 1,2,3. (Nm) |
| $D_{\mathrm{f}}$ | Bending stiffness of face plate (Nm) |
| $D_{Qx}$ | Transverse shear stiffness in $x$-direction (Nm) |
| $D_{Qy}$ | Transverse shear stiffness in $y$-direction (Nm) |
| $D_{\mathrm{w}}$ | Bending stiffness of web plate (Nm) |
| $E$ | Young's modulus (Pa) |
| $G$ | Shear modulus (Pa) |
| $M$ | Moment acting on laser weld (Nm) |
| $N_0$ | Buckling load per unit width (N) |
| $\nu$ | Poisson's ratio |
| $\theta_x$ | Rotation around $y$-axis |
| $\theta_y$ | Rotation around $x$-axis |
| $\theta_w$ | Rotation of the web plate around laser weld |
| $\theta_c$ | Deviation from the 90° angle at the T-joint |

## 1 Introduction

Steel sandwich plates are light-weight structures which can save space and improve safety; see Okazaki et al. [1]. They possess a high stiffness-to-weight and strength-to-weight ratio compared to conventional structures. This study concentrates on sandwich plates which consist of two face plates separated by web plates see Fig. 1(a). The connection between the web plates and face plates is achieved by laser stake welding which forms the T-joint. The thickness of the laser weld is typically less than that of the face plates and web plates; see Roland and Reinert [2]. This allows the ideally right angle of the T-joint to change when the sandwich plate is deformed transverse to the web plate direction. Therefore, the connection is not perfectly rigid, which results in the sandwich plate having a lower transverse shear stiffness. This has been found to have a high impact on the bending response, as presented in Romanoff et al. [3] for beams and Romanoff and Varsta [4] for plates.

The bending of a ship hull girder or bridge girder causes compression of its flanges; see Fig. 1(b). Buckling strength of the sandwich plate used at that location must be known due to in-plane loading. The laser-welded web-core sandwich plate may buckle in a local, global, or combined fashion. Up to now, the local buckling of the face plates has only been studied in a few studies; see Kolsters and Zenkert [5], Kolsters and Zenkert [6], and Kolsters [7]. Global buckling may become important for a slender sandwich plate; see Kozak [8]. However, none of these studies considered the actual laser weld rotation stiffness and its statistical variation. Haj-Ali et al. [9] and Rahman and Abubakr [10] showed for corrugated core plates that the connection between the face and the core has significant influence on buckling strength. Their investigation was based on three-dimensional (3-D) finite element method (FEM). In their work, they did not relate the resulting buckling strength to the transverse shear stiffness, even though Nordstrand [11] has shown that the buckling strength depends on the transverse shear stiffness of the corrugated plate.

The aim of this study is to investigate the influence of weld rotation stiffness on global buckling strength of web-core sandwich plates. Global buckling is in focus since it is dominant for a slender plate, for example when used in a ship or a bridge deck. Bifurcation buckling is studied since it fundamentally describes the buckling phenomenon and is part of structural design rules, e.g. DNV rules for ship classification [12]. Plate global buckling experiments do not exist that would validate the findings and thus the investigation is carried out with two theoretical methods that have different kinematical assumptions. The first is the equivalent single-layer (ESL) theory approach solved analytically for simply supported plates and numerically for clamped plates. First-order shear deformation theory is used. The second method is a 3-D FEM with shell elements for plates and spring elements for welds. Plates are loaded in their main load-carrying direction, i.e. parallel to the web plates. Four cross-sections of different properties are considered.

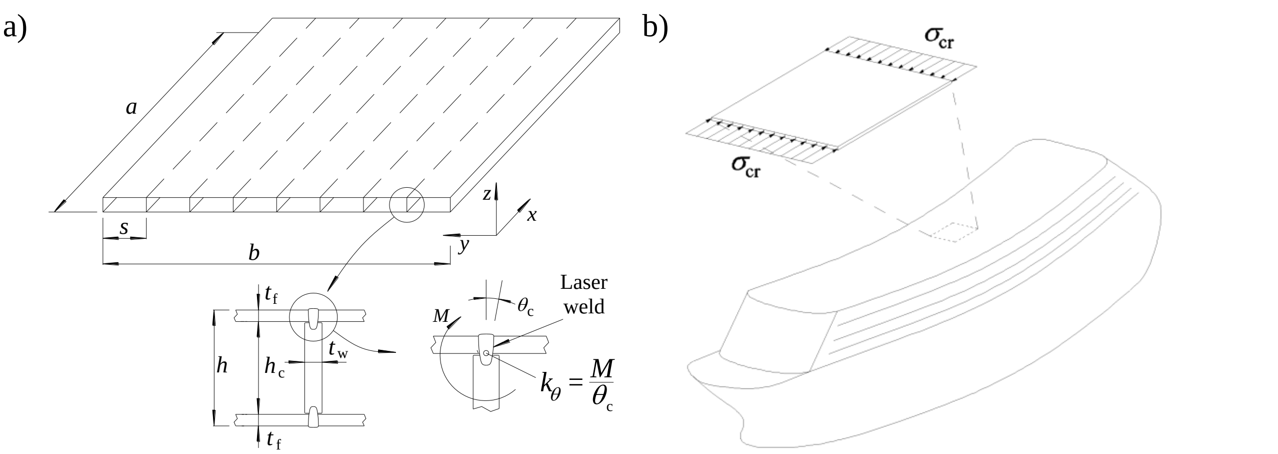


**Fig. 1.** *Laser-welded web-core sandwich plate (a) with the weld detail and (b) as a part of the ship hull girder.*

## 2 Analysis methods

### 2.1 Equivalent single-layer theory approach

The orthotropic sandwich plate is described through a single layer in its geometrical mid-plane. Equivalent stiffness properties for extension, coupling, bending and shear are described through *ABD*- and $D_Q$ –matrices, respectively; see Appendix. Laser weld rotation stiffness $k_\theta$ affects the transverse shear stiffness opposite to web-plate direction, which is given as [3]:

$$D_{Qy} = \frac{12D_w}{s^2\left(k_Q\left(\frac{D_w}{D_t}+6\frac{d}{s}\right)+12\frac{D_w}{k_\theta \cdot s}-2\frac{d}{s}\right)} \tag{1}$$

for which different stiffness parameters and $k_Q$ are presented in the Appendix. The laser weld rotation stiffness $k_\theta$ is defined as the ratio of the moment *M* to the rotation angle $\theta_c$ at the weld; see Fig. 2. :

$$k_\theta = \frac{M}{\theta_c}, \tag{2}$$

From Eq. (1) it is seen that the reduction of weld stiffness reduces the transverse shear stiffness.

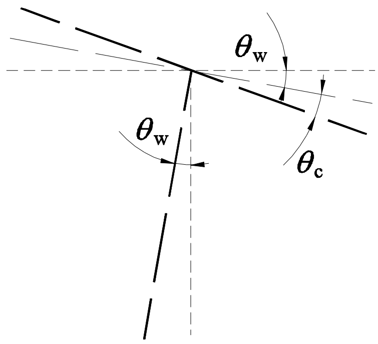


**Fig. 2.** *The angles around the weld [3]; the final deformed shape is shown with thick lines.*

### *2.1.1 Analytical solution for simply supported plates*

Symmetric laser-welded web-core sandwich plate is a special type of orthotropic plate where stiffness coefficients $A_{13}$, $A_{23}$, $D_{13}$, $D_{23}$ and $B_{ij}$ are equal to zero. The exact buckling load $N_0$ per unit width of a simply supported plate that follows the first-order shear deformation theory is given by Reddy [13] and Robinson [14]. The expression is presented in closed form:

$$N_0 = \frac{c_{33} + \left(\frac{\alpha^2}{D_{Qy}} + \frac{\beta^2}{D_{Qx}}\right)\cdot c_1}{\alpha^2 \cdot \left(1 + \frac{c_1}{D_{Qx}\cdot D_{Qy}} + \frac{c_2}{D_{Qx}} + \frac{c_3}{D_{Qy}}\right)}. \tag{3}$$

The coefficients are:

$\alpha = m\cdot\pi/a;$

$\beta = n\cdot\pi/b;$

$c_{33} = D_{11}\cdot\alpha^4 + 2\left(D_{12} + 2D_{33}\right)\alpha^2\beta^2 + D_{22}\beta^4;$

$c_1 = c_2\cdot c_3 - \left(c_4\right)^2;$

$c_2 = D_{11}\cdot\alpha^2 + D_{33}\cdot\beta^2;$

$c_3 = D_{33}\cdot\alpha^2 + D_{22}\cdot\beta^2;$

$c_4 = \left(D_{12} + D_{33}\right)\cdot\alpha\cdot\beta.$

Setting the shear stiffness to infinity, number of buckling half-waves in *y*-direction to one, and minimizing Eq. (3) with respect to *m*, gives the expression for isotropic steel plate buckling:

$$N_0 = \left( \frac{mb}{a} + \frac{a}{mb} \right)^2 \frac{\pi^2 \cdot D}{b^2}, \tag{4}$$

which is used in typical rules for ship structural design, additionally simplified for high aspect ratios, $a/b$, to

$$N_0 = 4\frac{\pi^2 \cdot D}{b^2}. \tag{5}$$

### *2.1.2 2-D FEM model*

The model consists of shell elements and presents the geometrical mid-plane of the plate, where also the loads and boundary conditions are described. The analyses are carried out using Abaqus software, version 6.6.1. Shell elements with four nodes (S4) are used.

Simply supported boundary condition is achieved by preventing the deflection $w$ and the rotation at a supported edge. Restrained rotation along $x$-axis is $\theta_x = dw/dx$ and similar notation is used for $y$-axis; see Fig. 3. Additional restraining of the rotation around the edge results in the clamped boundary condition. Symmetry conditions are not used since they would prevent certain buckling modes.

Plate width is divided in 100 elements. The element aspect ratio is close to unity. This was found to be sufficient in the initial study, because doubling it resulted in only a 0.2% difference in the buckling strength.

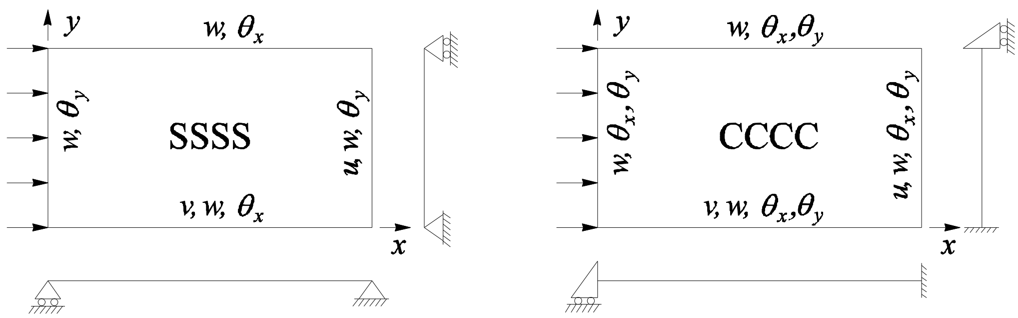


**Fig. 3.** *Boundary conditions for the 2-D model.*

## *2.2 3-D FEM model*

Face and web plates are modelled with shell elements to form an actual topology of the sandwich plate. The welds are modelled with spring elements which connect the face and web plates at their apparent intersection; see Fig. 4. The analyses are carried out using Ansys software, version 11.0. Shell element type 181 is used. For spring element, Combin 14 element is used. Concentrated nodal forces act on the nodes in the geometrical mid-plane.

To simply support or clamp the 3-D sandwich plate edge a different approach is required than for the 2-D mesh. This is due to the existence of the actual out-of-plane dimension. Therefore, the deflection restraint for the simply supported boundary condition is set only on the nodes at the geometrical mid-plane. This allows the rotation of the plate around the mid-plane edge. Furthermore, the vertical nodes along the edge are displaced equally in the edge direction to prevent the rotation of the in-plane axis orthogonal to the edge. For example, all the nodes at a certain web plate have the same displacement in the *y*-direction, *v*; see Fig. 4. To clamp the sandwich plate edge, vertical nodes at the edge displace equally parallel to the edge.

Four shell elements per web plate height and face plate width are used. The resulting mesh size for the studied cases was the maximum that could be solved with the available computing resources.

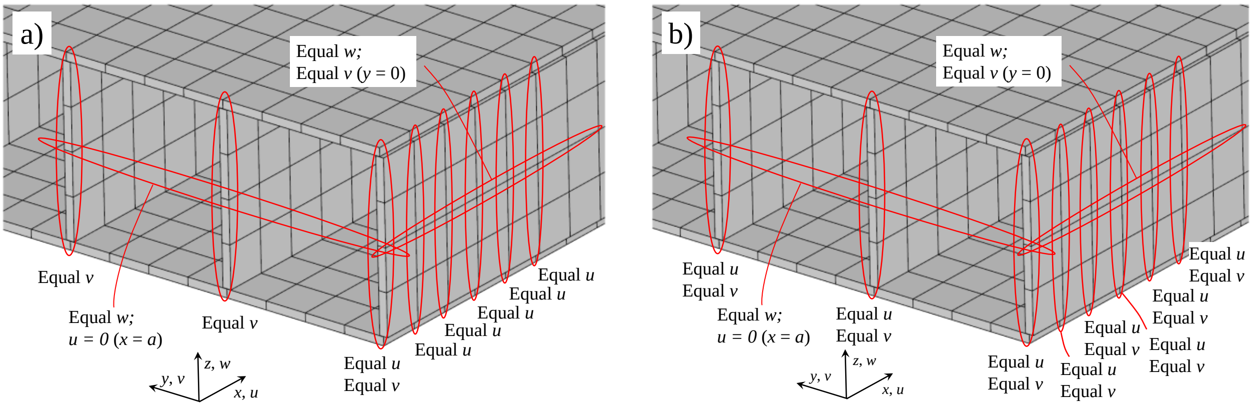


**Fig. 4.** *FE mesh and boundary conditions for 3-D model of a sandwich plate: a) simply supported and b) clamped.*

## 3 Case studies

### *3.1 Description of the studied plates*

The rotation stiffness of the laser weld was experimentally measured and presented by Romanoff et al. [3]. Their measurements were normally distributed with the average equal to $k_\theta$ = 107 kN and a standard deviation of 21 kN. The measured weld stiffness is used in buckling analysis in comparison to the case where the weld stiffness is not considered, i.e. it is infinite.

Four different cross-sections are studied. The notation used to identify the plates is the following: thickness of face plates × core height / web plate spacing. Thickness of the web plates is 4 mm for all plates. Case A (2.5×40/120) represents the standard sandwich configuration used in marine and civil applications. Case B (4×20/80) is a sandwich plate with thick face plates and small core height. Therefore, it is suitable for limited space requirements and high local loads e.g. from car tyres. Furthermore, it has high reduction of the transverse shear stiffness; see Eq. 1 and Table 1. In case C (4×80/80) the height of the core is increased, which results in considerable higher bending stiffnesses. In case D (1×80/80) the thickness of face plates has been reduced. Owing to this, the shear stiffness is decreased only by 6% when considering the average measured and infinite rotation stiffness. The properties of the cross-sections are given in Table 1. It can be seen that the transverse shear stiffness is a few orders of magnitude smaller than the longitudinal. The influence of weld rotation stiffness on transverse shear stiffness of the plates is presented in Fig. 5.

**Table 1.** *Properties of the plates. The ratio of $D_{22}$ to $D_{11}$ is shown in square brackets. The ratio of $D_{Qy}$ with finite and infinite $k_\theta$ is shown in round brackets.*

| Case | $t_f \times h_c$ / s [mm] | $D_{11}$ [kNm] | $D_{22}$ [kNm] | $D_{Qx}$ [kNm] | $D_{Qy}$ [kNm] | | | |
|---|---|---|---|---|---|---|---|---|
| | | | | | $k_\theta$ = 65 kN | $k_\theta$ = 107 kN | $k_\theta$ = 149 kN | $k_\theta = \infty$ kN |
| A | 2.5×40/120 | 548 | 511 [0.93] | $68 \cdot 10^3$ | 236 (0.56) | 285 (0.68) | 313 (0.75) | 419 |
| B | 4×20/80 | 268 | 261 [0.97] | $62 \cdot 10^3$ | 631 (0.22) | 908 (0.32) | 1123 (0.40) | 2830 |
| C | 4×80/80 | 3634 | 3195 [0.88] | $292 \cdot 10^3$ | 522 (0.36) | 698 (0.48) | 819 (0.56) | 1460 |
| D | 1×80/80 | 1182 | 743 [0.62] | $251 \cdot 10^3$ | 63 (0.91) | 65 (0.94) | 66 (0.96) | 69 |

Aspect ratios from 0.4 to 2.0 are studied. Plate width $b$ is fixed around seven metres and a maximum length $a$ restricted by current production capabilities to 14 m. The exact breadth of each sandwich plate is based on its web plate spacing $s$. The resulting dimensions are typical for ship structures. The material behaviour is described by a Young's modulus $E$ = 206 GPa and Poisson's ratio $\nu = 0.3$. The lowest eigenvalue is considered in analysis.

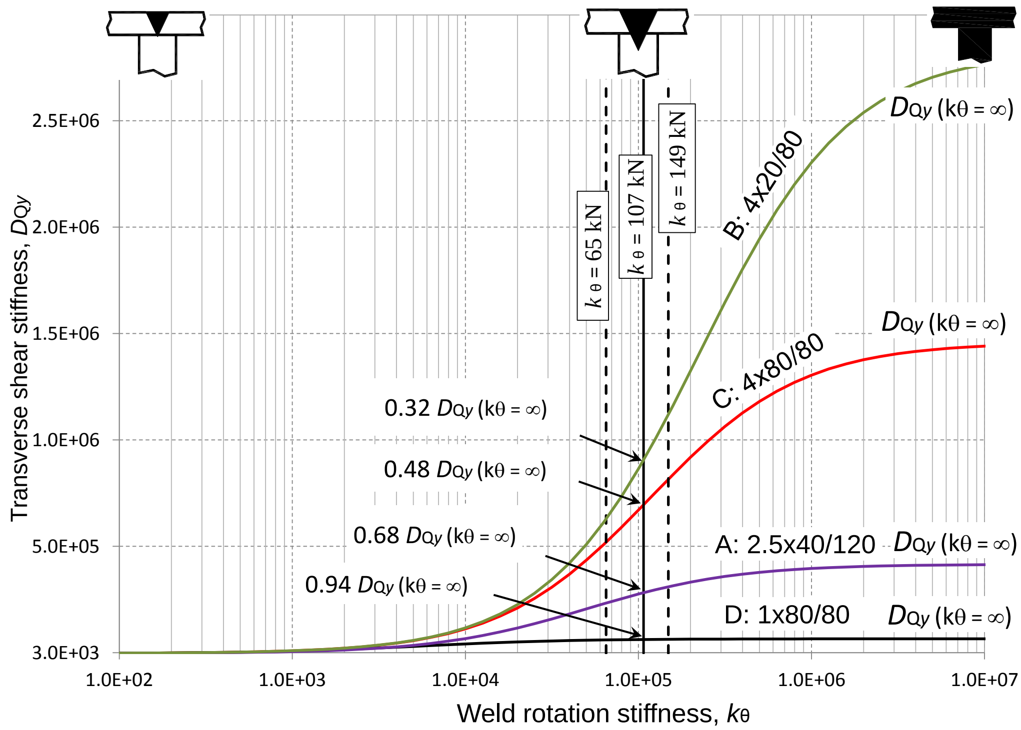


**Fig. 5.** *Transverse shear stiffness of plates vs. weld rotation stiffness.*

## 3.2 Results

Results of the buckling analysis are presented in Fig. 6. The load was multiplied with $b^2/(D_{11} \cdot \pi^2)$ to obtain a nondimensionalised form, called buckling coefficient $k$. The correspondence between ESL theory approach and 3-D FEM is excellent with both boundary conditions. 3-D FEM simulations are carried out for $a/b$ = 0.75, 1.00 and 1.50. Numerical solution with ESL theory approach is validated with the analytical expression.

All the plates show a reduction in buckling strength when the weld deformation is considered in analysis; see Fig. 6. The reduction is the smallest for the lowest aspect ratio and the largest at the point of buckling mode intersections. In that manner, the buckling strength for simply supported plate A (2.5×40/120) is reduced from 3% at $a/b$ = 0.4 to 8% at $a/b$ = 1.5 and it remains close to that value for higher aspect ratios. The most severe reduction was observed for case C (4×80/80), ranging from 5% for the smallest aspect ratio to 22% at $a/b$ = 1.5. In the case of sandwich plates B (4×20/80) and D (1×80/80) it is reduced by, on average, 3.5% and 1.5%, respectively.

The clamped plate shows a more severe reduction of buckling strength when compared to the simply supported plate. For case B, the difference is increased from 3.5% with simply supported to 11% with clamped edges. In the case of sandwich plate C, the difference ranges up to 24% (22% with simply supported edges) and for case A up to 12% (8%).

Furthermore, the intersection between the buckling modes has shifted towards higher aspect ratios. The shift is especially pronounced for clamped plates, where in case C the intersection between the first and the second buckling mode is moved from $a/b$ = 1.45 to $a/b$ = 1.8 (24%).

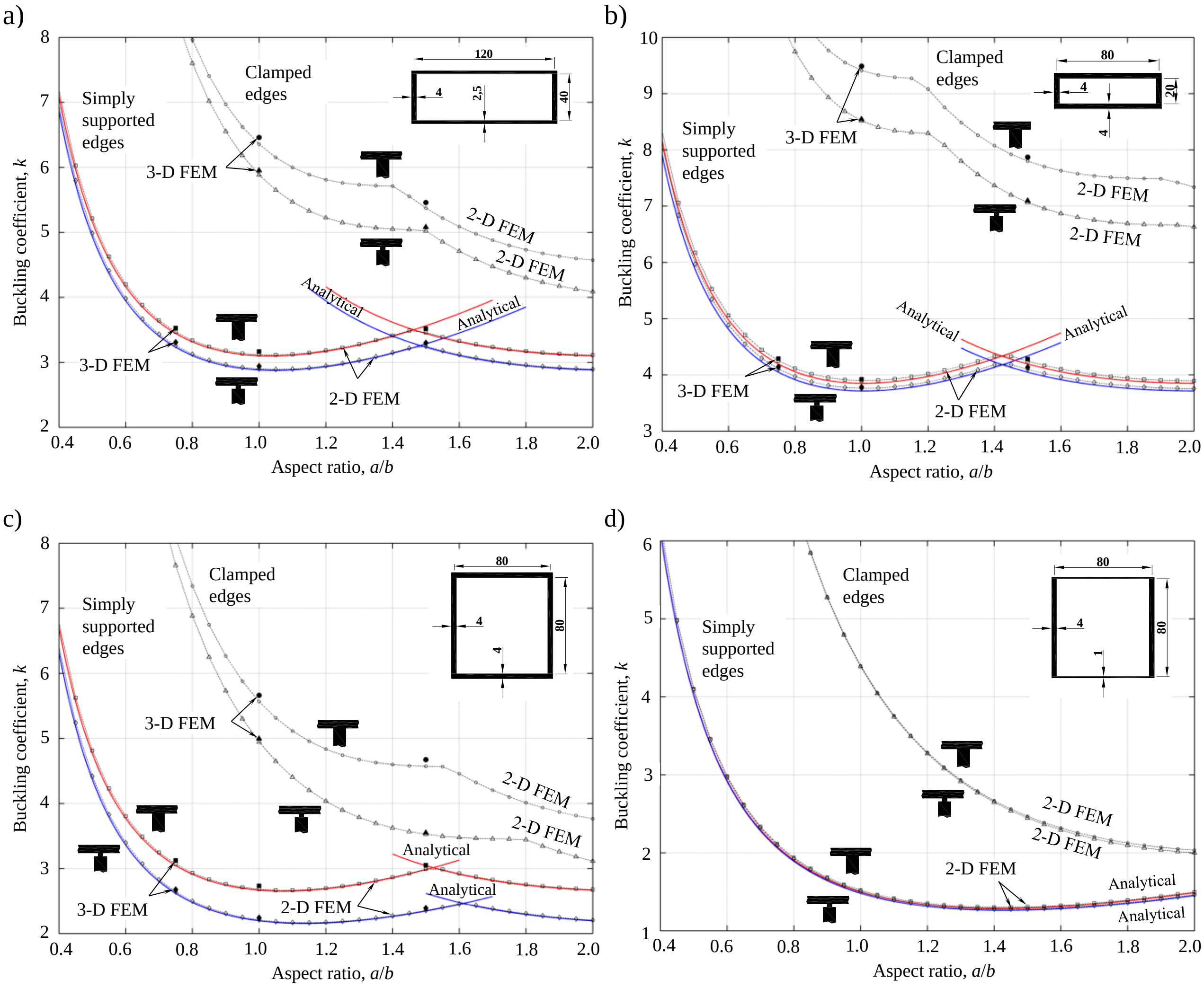


**Fig. 6.** *(a) – (d) Buckling coefficient versus plate aspect ratio, with and without taking joint stiffness into account.*

### 3.2.1 *Variation of rotation stiffness*

An additional decrease in the buckling strength for all the cross-sections occurs for $k_\theta$ = 65 kN, which is the value of the average rotation stiffness minus two standard deviations. This is the lower bound of the weld stiffness measurements with the confidence of 95%. Fig. 7(a) presents the reduction for the simply supported plate C, which is affected the most. The differences in buckling strength between cases $k_\theta = \infty$ kN and $k_\theta$ = 65 kN are from 7% to 30%.

Exposure of the plates to sea water could lead to weld thickness reduction due to corrosion; see Jelovica et al. [15] and Aromaa et al. [16]. The weld stiffness would decrease from experimentally measured values. The shift of buckling mode intersections is in that case so significant that the first half-wave dominates even at high aspect ratios. Fig. 7(b) presents the buckling coefficient for the simply supported plates with $a$ = 14 m and $b$ = 4 m, thus $a/b$= 3.5. Plate production favours such dimensions. It can be seen from the figure that the plates buckle in single-half wave mode for very low weld rotation stiffness, respectively the shear stiffness. The buckling strength is severely decreased.

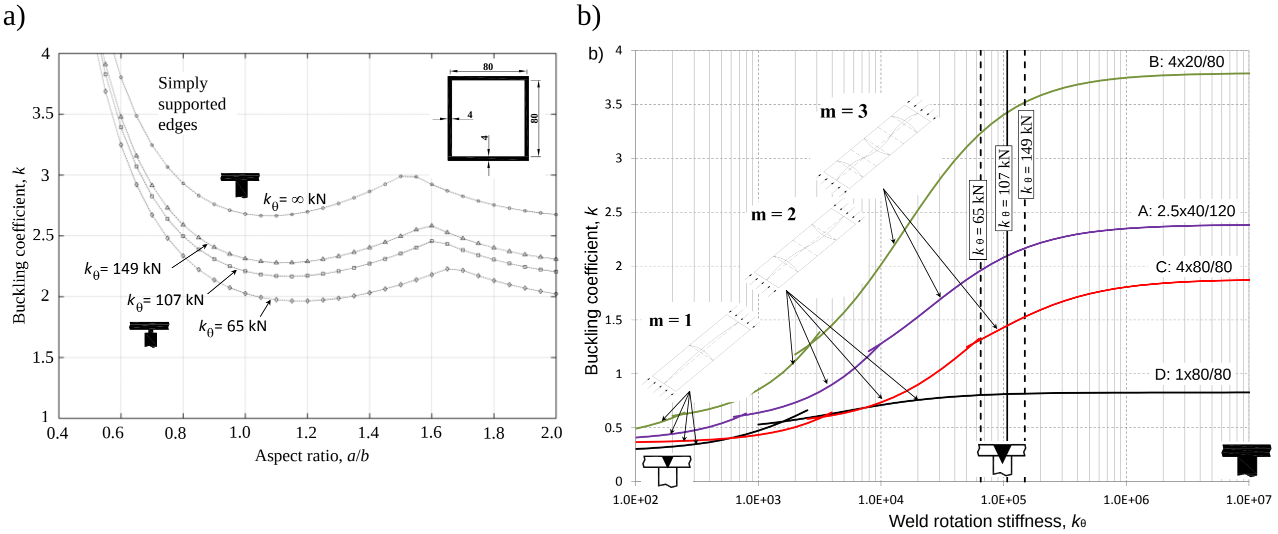


**Fig. 7.** *(a) Buckling coefficient for simply supported plate C with $k_\theta = \infty$, 149, 107, and 65 kN; (b) Buckling coefficient versus weld rotation stiffness for simply supported plates of aspect ratio 3.5.*

## 4 Discussion and conclusions

The weld rotation stiffness was found to have significant influence on the buckling strength. For case C (4×80/80), where the reduction in transverse shear stiffness is second highest and the bending stiffness is the highest, the reduction of the buckling strength was 22% and 24% at maximum for simply supported and clamped edges. This reduction was obtained by lowering the weld stiffness from infinite to the average measured value from Romanoff et al. [3]. This finding is in line with those presented in Romanoff and Varsta [4] for the plate bending. The typical plate for marine applications (2.5×40/120) showed an 8% difference between the average and the infinite weld stiffness. The smallest reduction, of 1.5%, was observed for case D (1×80/80), which has thin face plates and whose transverse shear stiffness is only reduced by 6%.

For the same weld stiffness variation, plates showed different buckling strength reduction. The reduction of strength cannot be solely attributed to the transverse shear stiffness decrease. This can be concluded from comparison of cases B and C. The transverse shear stiffness was reduced the most in case B, however, the buckling strength was decreased by only 3.5% for simply supported edges. On the other hand, case C features second highest reduction of transverse shear stiffness, however, the buckling strength was decreased by 22%. Buckling strength in case B is governed by $c_{33}$ term in Eq. (1) and thus the changes in $D_{Qy}$ do not have significant effect. On the other hand, in case C the $c_1$ and $c_3$ coefficients increase and it results in higher influence of transverse shear stiffness. This effect is due to the higher sandwich plate bending stiffness in case C, i.e. increased core height. Thus, the strength is affected more in plates with high transverse shear stiffness reduction and high bending stiffness.

In general, clamped plate edges resulted in more severe decrease of buckling strength, due to larger effect of shear deformation. Thus, the weakness of the connection between the face plate and the web plate became more evident. For case B, the reduction in strength is increased from 3.5% for simply supported edges to 11% for clamped edges.

Furthermore, it was found that a reduction in the weld stiffness shifts the intersections of buckling modes towards higher aspect ratios. This is in line with the findings from Nordstrand [11] for corrugated plates. Additionally, in the case of very low weld stiffness the sandwich plate buckled in a single half-wave mode even at high plate aspect ratios. The buckling strength was severely decreased. Such case could occur for plates with decreased weld thickness due to corrosion; see Jelovica et al. [15] and Aromaa et al [16], and due to fatigue; see Frank [17].

Shift of buckling mode intersections could be important for practical design where the spans between the plate supports are fixed and the aspect ratio is in the range 1-3. Because of typically small aspect ratios, the design of sandwich plate cannot be simplified by using the buckling coefficient, such as for isotropic steel plate, where it equals 4 for long plates. The results of this study show the importance of considering the weld in buckling analysis. Further investigation should include more realistic material properties. Based on these investigations, buckling experiments can be planned and carried out for sandwich plates in the future.

## Appendix – Stiffness properties

The extensional, extensional-bending, and bending stiffness matrices respectively are (see Romanoff and Varsta [4])

$$\left([A],[B],[D_0]\right)=\int_{-h/2}^{h/2}[E]_i\left(1,d_i,d_i z\right)dz,\;\; i=\mathrm{t,c,b} \tag{6}$$

and the local bending stiffness of the face plates is

$$\begin{aligned}[D]_\mathrm{t}&=\frac{t_\mathrm{t}^{\,3}}{12}[E]_\mathrm{t}\,,\\ [D]_\mathrm{b}&=\frac{t_\mathrm{b}^{\,3}}{12}[E]_\mathrm{b}\,,\end{aligned} \tag{7}$$

where the distance from the mid-plane of the plate is

$$d_{\mathrm{t}} = \frac{h}{2} - \frac{t_{\mathrm{t}}}{2},$$
$$d_{\mathrm{c}} = z, \tag{8}$$
$$d_{\mathrm{b}} = -\frac{h}{2} + \frac{t_{\mathrm{b}}}{2}.$$

The elasticity matrix [$E$] of the face plates is

$$\left[E\right]_i = \frac{1}{1-\nu_i^2}\begin{bmatrix} E_i & \nu_i E_i & 0 \\ \nu_i E_i & E_i & 0 \\ 0 & 0 & G_i\left(1-\nu_i^2\right) \end{bmatrix}, \quad i = \mathrm{t,b}, \tag{9}$$

while the core has the elasticity matrix

$$\left[E\right]_{\mathrm{c}} = \frac{E_{\mathrm{w}} t_{\mathrm{w}}}{s}\begin{bmatrix} 1 & 0 & 0 \\ 0 & 0 & 0 \\ 0 & 0 & 0 \end{bmatrix}. \tag{10}$$

The shear stiffness in the longitudinal direction is

$$D_{Q\mathrm{x}} = k_{11}^2\left( G_{\mathrm{t}} t_{\mathrm{t}} + G_{\mathrm{b}} t_{\mathrm{b}} + \frac{t_{\mathrm{w}}}{s} G_{\mathrm{w}} h_{\mathrm{c}} \right), \tag{11}$$

where

$$k_{11} = \sqrt{\frac{1}{A\left( \sum_i \int \left( \frac{\tau_i}{Q_{Q\mathrm{x}} s} \right)^2 t_i \mathrm{d}s_i \right)}}, \quad i = \mathrm{t,c,b}, \tag{12}$$

$$k_Q = \frac{1 + 12\frac{D_{\mathrm{t}}}{s}\left( \frac{1}{k_\theta^{\mathrm{t}}} - \frac{1}{k_\theta^{\mathrm{b}}} \right) + 6\frac{D_{\mathrm{t}}}{D_{\mathrm{w}}}\frac{d}{s}}{1 + 12\frac{D_{\mathrm{t}}}{D_{\mathrm{w}}}\frac{d}{s} + \frac{D_{\mathrm{t}}}{D_{\mathrm{b}}}}. \tag{13}$$

The shear stiffness in the transverse direction $D_{Q\mathrm{y}}$ is given by Eq. (1).

## Acknowledgements

The work was founded by EU research project SANDWICH, Aalto University Post Doc, SUTERA project and the Finnish National Graduate School in Engineering Mechanics. This financial support is gratefully acknowledged.

## References

[1] Okaziki T, Siljenberg BJ, Shield CK, Mantell SC. Web crippling strength of a steel sandwich panel with V-shaped webs. Journal of Constructional Steel Research 2009; 65:1721-1730.

[2] Roland F, Reinert T. Laser welded sandwich panels for the ship building industry. Lightweight construction – latest developments 2000; SW1:1-17.

[3] Romanoff J, Remes H, Socha G, Jutila M, Varsta P. The stiffness of laser stake welded T-joints in web-core sandwich structures. Thin-Walled Structures 2007; 45(4):453–462.

[4] Romanoff J, Varsta P. Bending response of web-core sandwich plates. Composite Structures 2007; 81(2):292-302.

[5] Kolsters H, Zenkert D. Buckling of laser-welded sandwich panels: Part 1: elastic buckling parallel to the webs. Journal of Engineering for the Maritime Environment 2006; 220(2):67-79.

[6] Kolsters H, Zenkert D. Buckling of laser-welded sandwich panels: Part 2: elastic buckling normal to the webs. Journal of Engineering for the Maritime Environment 2006; 220(2):81-94.

[7] Kolsters H. Structural Design of Laser-Welded Sandwich Panels for Marine Applications. Doctoral Dissertation, Royal Institute of Technology, Department of Aeronautical and Vehicle Engineering, Stockholm 2004. Paper D: Buckling of laser-welded sandwich panels: Part 3: Ultimate strength and experiments.

[8] Kozak J. Problems of strength modeling of steel sandwich panels under in-plate loads. Polish Maritime Research 2006; S1:9-12.

[9] Haj-Ali R, Choi J, Wei B, Popil R, Schaepe M. Refined nonlinear finite element models for corrugated fiberboards. Composite Structures 2009; 87:321-333.

[10] Rahman AA, Abubakr S. A finite element investigation of the role of adhesive in the buckling failure of corrugated fiberboard. Wood and Fiber Science 2004; 36(2):260-268.

[11] Nordstrand T. On buckling loads for edge-loaded orthotropic plates including transverse shear. Composite structures 2004; 65:1-6.

[12] Det Norske Veritas. Rules for the classification of steel ships. Høvik, 2005.

[13] Reddy JN. Mechanics of laminated composite plates and shells – Theory and analysis: second ed. Boca Raton: CRC Press, 2000.

[14] Robinson JR. The Buckling and Bending of Orthotropic Sandwich Panel With All Edges Simply-Supported. The Aeronautical Quarterly 1955: 125-148.

[15] Jelovica J, Romanoff J, Ehlers S, Aromaa J. Ultimate strength of corroded web-core sandwich beams. Submitted to Marine Structures Journal.

[16] Aromaa J, Leino J, Pehkonen A, Virtanen J. Corrosion of steel cell structures in seawater. Aalto University series TT 8/2011, 2011.

[17] Frank D, Remes H, Romanoff J. Fatigue assessment of laser stake-welded T-joints. International Journal of Fatigue 2011; 33:102-114.